Paper # 070RK-0195 **Topic: Reaction Kinetics**

8th US National Combustion Meeting
Organized by the Western States Section of the Combustion Institute
and hosted by the University of Utah
May 19–22, 2013.

Reduced mechanisms for gasoline surrogates valid at engine conditions

Kyle E. Niemeyer[1,2] *Chih-Jen Sung*[2]

[1]*Department of Mechanical and Aerospace Engineering, Case Western Reserve University, Cleveland, OH*

[2]*Department of Mechanical Engineering, University of Connecticut, Storrs, CT*

A detailed mechanism for four-component gasoline surrogates, developed by Lawrence Livermore National Laboratory (LLNL), showed good agreement with experiments in engine-relevant conditions. However, with 1389 species and 5935 reversible reactions, the mechanism is far too large to use in practical engine simulations. Therefore, reduction of the mechanism was performed. First, the directed relation graph with error propagation and sensitivity analysis (DRGEPSA) method was used to generate skeletal mechanisms at varying levels of detail. This step produced significantly reduced skeletal mechanisms, but those with tight error limits were still too sizable for practical use. Therefore, a second reduction step was employed, using the quasi-steady-state (QSS) approximation based on computational singular perturbation (CSP) analysis. The QSS species concentrations were solved analytically, rather than through an iterative solution approach. For error constraints of 10% and 30%, the final reduced mechanisms consist of 245 and 178 species, respectively. Both reduced mechanisms (and the corresponding skeletal mechanisms) were validated with homogeneous autoignition simulations over engine-relevant conditions, and both showed good agreement in predicting ignition delay.

1 Introduction

Modeling the kinetics of gasoline—as well as other liquid transportation fuels—is complex due to the near-continuous spectrum of constituent hydrocarbons. One widely used solution in the combustion community is to use surrogate fuels that consist of a small number of hydrocarbons representing the major hydrocarbon classes present in real gasoline. Historically, binary blends of *n*-heptane and *iso*-octane were used to model gasoline at various octane numbers; these are the primary reference fuels (PRFs). However, these simple mixtures in general can't match the physical properties of gasoline. For example, the H/C ratio of gasoline is usually less than two [1], but PRFs are limited to the range of 2.3–2.25. In addition, PRFs can't capture the so-called gasoline "sensitivity," the difference between motor octane number (MON) and research octane number (RON); RON and MON are equal for any PRF.

In order to better match the physical and kinetic properties of gasoline, a number of research groups developed surrogate formulations with additional components to represent other major hydrocarbon classes (e.g., olefins, aromatics). Gauthier et al. [2] and Chaos et al. [1] proposed three-component surrogates, adding toluene to *n*-heptane and *iso*-octane to form toluene reference

fuels (TRFs). Recently, Mehl et al. [3, 4] proposed a four-component gasoline surrogate consisting of *n*-heptane, *iso*-octane, toluene, and 2-pentene to represent linear hydrocarbons, branched hydrocarbons, aromatics, and olefins, respectively. They found that this surrogate emulates engine data, laminar flame speeds, and shock tube ignition delay times of the target gasoline with good agreement. Kukkadapu et al. [5] performed further experimental and computational validation of the surrogate mixture and representative kinetic mechanism of Mehl et al. [3]. They found that for stoichiometric mixtures the surrogate matched the autoignition response of gasoline in a rapid compression machine, and the mechanism predicted overall ignition delays of real gasoline with good agreement.

While the performance of the proposed mechanism for gasoline surrogates is promising, the large size (1389 species and 5936 reversible reactions) poses a significant challenge to practical engine simulations. The computational cost of chemistry scales by the third power of the number of species in the worst case [6]. Chemistry calculations must be performed at least once for each grid point or cell, and three-dimensional, high-fidelity simulations of engines or combustion chambers could require mesh sizes of 10^4–10^7 cells. Significant reduction in mechanism size is therefore vital in order to use the mechanism in practical simulations.

A number of mechanism reduction methods have been developed in recent years to counter the trend of increasing mechanism sizes, as reviewed by Lu and Law [6]. Most focus on identifying and removing unimportant species, or performing "skeletal" reduction. Many methods have been developed, but one class that received significant development is that based on the directed relation graph (DRG) [7–9]. Based on the graphical representation of reaction pathways of Bendtsen et al. [10], DRG quantifies the importance of species using normalized contributions to the overall production rates of certain preselected important, "target" species. Since the introduction of DRG, a number of more effective variants have been developed, including DRG-aided sensitivity analysis (DRGASA) [11–13], DRG with error propagation (DRGEP) [14, 15], DRGEP with sensitivity analysis (DRGEPSA) [16], and path-flux analysis [17].

Another reduction paradigm focuses on time-scale analysis, identifying and removing short times scales—induced by rapidly depleting species and/or fast reversible reactions—that cause chemical stiffness. Many methods rely on the classical quasi-steady state (QSS) [18, 19] and partial equilibrium approximations [20, 21], which replace differential equations with algebraic relations for some species. Originally, such species and reactions were identified on the basis of experience, but systematic methods that use analysis of the Jacobian matrix to identify QSS species and PE reactions, namely the computational singular perturbation (CSP) [22–24] and intrinsic low-dimensional manifold [25] methods, have since been developed.

Finding a single skeletal reduction not sufficient to reduce the size of large detailed mechanisms, Lu and Law [13] presented a multi-stage reduction strategy and applied it to to a detailed mechanism for *n*-heptane. Their approach consisted of DRGASA, unimportant reaction elimination, isomer lumping, and time scale reduction through the QSS approximation. In addition, they grouped similar diffusive species in the final reduced mechanism to reduce the cost of the mixture-averaged diffusion formulation. Later, Niemeyer et al. [16] showed that DRGEPSA can produce more compact skeletal mechanisms for the same level of accuracy than DRG, DRGEP, and DRGASA.

In this work, we apply a multi-stage reduction strategy similar to that developed by Lu and Law

[13] based on DRGEPSA to the large detailed mechanism for gasoline surrogates of Mehl et al. [3, 4]. First, the DRGEPSA method is applied to remove a large number of unimportant species (and corresponding reactions). Second, a step of further unimportant reaction elimination is performed to remove additional reactions—this step doesn't affect the number of species, but the complexity of the mechanism is reduced. Third, QSS species are identified using CSP analysis. Finally, an analytic solution for the QSS species concentrations is generated. We then validate the resulting reduced mechanisms over engine-relevant conditions, comparing the performance against that of the detailed mechanism in predicting global phenomena such as homogeneous, adiabatic ignition delay and extinction. In addition, we perform local comparisons of major species profiles, emissions, and CA ignition prediction in HCCI engine simulations.

2 Methodology

2.1 DRGEP

In the current work we use the DRGEPSA method of Niemeyer et al. [16], which is based on the DRGEP of Pepiot-Desjardins and Pitsch [14] followed by a sensitivity analysis of remaining species. First, the DRGEP method is described here in brief; further detail can be found in our prior work [15, 16]. Accurate calculation of the production of a species A that is strongly dependent on another species B requires the presence of species B in the reaction mechanism. This dependence is expressed with the direct interaction coefficient (DIC):

$$r_{AB} = \frac{\left|\sum_{i=1}^{N_R} \nu_{A,i}\Omega_i\delta_B^i\right|}{\max\left(P_A, C_A\right)}, \tag{1}$$

where

$$P_A = \sum_{i=1}^{N_R} \max\left(0, \nu_{A,i}\Omega_i\right), \tag{2}$$

$$C_A = \sum_{i=1}^{N_R} \max\left(0, -\nu_{A,i}\Omega_i\right), \tag{3}$$

$$\delta_B^i = \begin{cases} 1 & \text{if reaction } i \text{ involves species } B, \\ 0 & \text{otherwise,} \end{cases} \tag{4}$$

A and B represent the species of interest (with dependency in the $A \rightarrow B$ direction meaning that A depends on B), i the ith reaction, $\nu_{A,i}$ the overall stoichiometric coefficient of species A in the ith reaction ($\nu_{A,i} = \nu''_{A,i} - \nu'_{A,i}$), Ω_i the overall reaction rate of the ith reaction, and N_R the total number of reactions.

After calculating the DIC for all species pairs, a graph search is performed—using Dijkstra's algorithm as described by Niemeyer and Sung [15]—starting at user-selected target species to find the dependency paths for all species from the targets. A path-dependent interaction coefficient (PIC) represents the error propagation through a certain path and is defined as the product of intermediate

DICs between the target T and species B through pathway p:

$$r_{TB,p} = \prod_{j=1}^{n-1} r_{S_j S_{j+1}}, \tag{5}$$

where n is the number of species between T and B in pathway p and S_j is a placeholder for the intermediate species j starting at T and ending at B. An overall interaction coefficient (OIC) is then defined as the maximum of all PICs between the target and each species of interest:

$$R_{TB} = \max_{\text{all paths } p} \left(r_{TB,p}\right). \tag{6}$$

Pepiot-Desjardins and Pitsch [14] also proposed a coefficient scaling procedure to better relate the OICs from different points in the reaction system evolution that we adopt here. A pseudo-production rate of a chemical element a based on the production rates of species containing a is defined as

$$P_a = \sum_{\text{all species } S} N_{a,S} \max\left(0, P_S - C_S\right), \tag{7}$$

where $N_{a,S}$ is the number of atoms a in species S and P_S and C_S are the production and consumption rates of species S as given by Eqs. (2) and (3), respectively. The scaling coefficient for element a and target species T at time t is defined as

$$\alpha_{a,T}(t) = \frac{N_{a,T}\left|P_T - C_T\right|}{P_a}. \tag{8}$$

For the set of elements $\{\mathscr{E}\}$, the global normalized scaling coefficient for target T at time t is

$$\alpha_T(t) = \max_{a\in\{\mathscr{E}\}} \left(\frac{\alpha_{a,T}(t)}{\max\limits_{\text{all time}} \alpha_{a,T}(t)} \right). \tag{9}$$

Given a set of kinetics data $\{\mathscr{D}\}$ and target species $\{\mathscr{T}\}$, the overall importance of species S to the target species set is

$$\overline{R_S} = \max_{\substack{T\in\{\mathscr{T}\} \\ k\in\{\mathscr{D}\}}} \left[\max_{\text{all time},\, k} \left(\alpha_T R_{TS}\right) \right]. \tag{10}$$

The removal of species where $\overline{R_S} < \varepsilon_{\text{EP}}$ is considered negligible to the overall production/consumption rates of the target species and therefore such species are unimportant for the given conditions and can be removed from the reaction mechanism. The optimal threshold ε_{EP} is chosen in an iterative manner. Starting with a low value (e.g., 0.01), an initial skeletal mechanism is generated and the error in ignition delay prediction (compared to the detailed mechanism) is calculated for all initial conditions using the following:

$$\delta_{\text{skel}} = \max_{k\in\{\mathscr{D}\}} \frac{\left|\tau^k_{\text{det}} - \tau^k_{\text{skel}}\right|}{\tau^k_{\text{det}}}, \tag{11}$$

where τ^k_{det} and τ^k_{skel} are the ignition delays calculated by the detailed and skeletal mechanisms, respectively, and $\{\mathscr{D}\}$ is the set of autoignition initial conditions. If the maximum error for this initial skeletal mechanism is above the user-specified error limit δ_{limit}, the threshold is decreased. For this and any subsequent mechanisms, if the maximum error is below the error limit the threshold is increased until the error reaches the specified limit. This procedure generates a minimal skeletal mechanism using DRGEP for a given error limit prior to application of sensitivity analysis.

2.2 Sensitivity analysis

Following the removal of a large number of species by the DRGEP method, a sensitivity analysis algorithm eliminates additional unimportant species. Species with overall importance values $\left(\overline{R_S}\right)$ that satisfy $\varepsilon_{EP} < \overline{R_S} < \varepsilon^*$, where ε^* is a higher value (e.g., 0.1–0.4), are classified as "limbo" species to be analyzed for removal. Species where $\overline{R_S} > \varepsilon^*$ are classified as "retained" species and included in the final skeletal mechanism. Previously used sensitivity analysis approaches removed limbo species one-by-one, arranged them in ascending order based on the error induced to the mechanism by removal, then removed using this order until the global error reached a limit [11–13, 16, 26, 27].

The sensitivity analysis algorithm first evaluates the error induced by the removal of each species, given by

$$\delta_S = \left|\delta_{S,\text{ind}} - \delta_{\text{skel}}\right|, \tag{12}$$

where δ_{skel} is the error of the current skeletal mechanism (prior to temporary removal of species S) and $\delta_{S,\text{ind}}$ the error induced by the removal of species S, by removing each one-by-one. Then, using the criterion given by Eq. (12) the algorithm sorts the species for removal in ascending order of induced error. Species are removed in order until the maximum error reaches the user-specified limit. By using δ_S rather than $\delta_{S,\text{ind}}$, the species whose removal affects the mechanism the least is selected for removal.

2.3 Unimportant reaction elimination

After the DRGEPSA method generates a skeletal mechanism, an additional step of further unimportant reaction elimination is performed based on the methodology of Lu and Law [13]. Using an approach based on the CSP importance index [29], the normalized contribution of a reaction i to the production rate of a species A is

$$I_{A,i} = \frac{\left|\nu_{A,i}\Omega_i\right|}{\sum_{j=1,N_R}\left|\nu_{A,j}\Omega_j\right|}, \tag{13}$$

where a reversible reaction must be treated as a single reaction [13]. Reactions are considered unimportant if $I_{A,i} < \varepsilon_{\text{reac}}$ for all species A; in other words, if

$$\max_{\text{all species } A} I_{A,i} \geq \varepsilon_{\text{reac}}, \tag{14}$$

reaction i is retained in the mechanism. The threshold $\varepsilon_{\text{reac}}$ is determined iteratively based on a user-defined error limit in a similar manner to ε_{EP}.

2.4 QSS species identification

Our approach for identifying global QSS species is based on the CSP analysis of Lam and coworker [22–24, 30], and follows the same approach as Lu and Law [13, 31].

$$\frac{d\mathbf{y}}{dt} = \mathbf{g}(\mathbf{y}) \tag{15}$$

$$\frac{d\mathbf{g}}{dt} = \mathbf{J}\mathbf{g}, \quad \mathbf{J} \equiv \frac{d\mathbf{g}}{d\mathbf{y}} \tag{16}$$

CSP analysis decomposes the source terms $\mathbf{g}$ into "modes" using basis vectors:

$$\mathbf{f} = \mathbf{B}\mathbf{g}, \tag{17}$$

$$\frac{d\mathbf{f}}{dt} = \mathbf{\Lambda}\mathbf{f}, \tag{18}$$

$$\mathbf{\Lambda} = \left(\frac{d\mathbf{B}}{dt} + \mathbf{B}\mathbf{J}\right)\mathbf{A}, \tag{19}$$

$$\mathbf{A} = \mathbf{B}^{-1}, \tag{20}$$

where the matrices $\mathbf{A}$ and $\mathbf{B}$ hold the column and row basis vectors, respectively, and $\mathbf{f}$ is the vector of modes.

Practically, this procedure is implemented by calculating the Jacobian $\mathbf{J}$ using finite differences, then using LAPACK subroutine DGEEV [32] to calculate the eigenvalues and eigenvectors. The Jacobian is assumed to be time independent such that the basis rotation term $\frac{d\mathbf{B}}{dt} = 0$, and as a result Eq. (19) becomes

$$\mathbf{\Lambda} = \mathbf{B}\mathbf{J}\mathbf{A}, \tag{21}$$

or

$$\mathbf{J} = \mathbf{A}\mathbf{\Lambda}\mathbf{B}, \tag{22}$$

where the diagonal elements of $\mathbf{\Lambda}$ are the eigenvalues of $\mathbf{J}$, the columns of $\mathbf{A}$ contain the right eigenvectors, and the rows of $\mathbf{B}$ contain the left eigenvectors.

Next, the fast and slow subspaces are separated, such that

$$\frac{d}{dt}\begin{pmatrix}\mathbf{f}^{\text{fast}} \\ \mathbf{f}^{\text{slow}}\end{pmatrix} = \begin{pmatrix}\mathbf{\Lambda}^{\text{fast}} & \\ & \mathbf{\Lambda}^{\text{slow}}\end{pmatrix}\begin{pmatrix}\mathbf{f}^{\text{fast}} \\ \mathbf{f}^{\text{slow}}\end{pmatrix}. \tag{23}$$

The fast modes are those that exhaust rapidly and decay quickly, while the slow modes remain important and control the overall behavior of the system. The eigenvalues associated with fast modes, the diagonal elements of $\mathbf{\Lambda}^{\text{fast}}$, are negative with a much larger magnitude than the eigenvalues associated with the slow modes, contained in $\mathbf{\Lambda}^{\text{slow}}$. The separation of the fast and slow subspaces is identified by a timescale analysis:

$$\frac{-1}{\lambda_{\min}\left(\mathbf{\Lambda}^{\text{fast}}\right)} \equiv \tau_{\text{fast}} < \frac{\tau_{\text{c}}}{\alpha_{\text{CSP}}} \tag{24}$$

where the time scale of the fast subspace, τ^{fast}, is the negative inverse of the smallest magnitude eigenvalue in $\mathbf{\Lambda}^{\text{fast}}$, τ_c is a characteristic time scale of the reacting system (here, autoignition delay), and α_{CSP} is a safety factor (e.g., 10–100).

Once the fast and slow subspaces are separated, the species rates of production can be projected onto the two subspaces:

$$\mathbf{g} = \left(\mathbf{Q}^{\text{fast}} + \mathbf{Q}^{\text{slow}}\right)\mathbf{g}, \tag{25}$$

where the fast and slow projection matrices are

$$\mathbf{Q}^{\text{fast}} = \mathbf{A}^{\text{fast}}\mathbf{B}^{\text{fast}}, \quad \mathbf{Q}^{\text{slow}} = \mathbf{A}^{\text{slow}}\mathbf{B}^{\text{slow}}, \tag{26}$$

respectively. The *i*th species is considered QSS if it satisfies the following condition over the entire parameter range of interest:

$$\left|\mathbf{Q}^{\text{slow}}_{\text{i,i}}\right| < \varepsilon_{\text{CSP}}, \tag{27}$$

where $\mathbf{Q}^{\text{slow}}_{\text{i,i}}$ is the *i*th diagonal element of $\mathbf{Q}^{\text{slow}}$ and ε_{CSP} is a small threshold value.

2.5 Analytical QSS solution

Once the set of QSS species are selected, applying the QSS approximation results in a set of nonlinear algebraic equations for the concentrations of each species, coupled with the remaining differential equations governing the non-QSS species. Past efforts focused on solving this system of equations through iterative schemes, but convergence difficulties can arise due to deterioration of the QSS assumption, leading to excessive computational cost [33]. An alternative is to linearize the relations—assuming the coupling between QSS species is sparse in general—and generate an analytical solution for the concentrations of the QSS species. Here, we present our methodology for this, adopted from the approach established by Lu and Law [34], who also presented greater detail and explanation of this method. We summarize the necessary steps here.

First, we must ensure the contribution of the nonlinear terms in the QSS equations is negligible such that these terms can be eliminated from the relations. According to the QSS approximation, the net production rate of a QSS species is small compared to both the production and consumption rates. This approximation results in a system of equations for the QSS species:

$$\omega_{\text{P},i} = \omega_{\text{C},i} \quad i = 1, 2, \ldots, N \tag{28}$$

with the species production and consumption rates expressed as

$$\omega_{\text{P},i} = \sum_{j=1}^{N_R} \nu''_{i,j}\Omega_j \quad \text{and} \quad \omega_{\text{C},i} = \sum_{j=1}^{N_R} \nu'_{i,j}\Omega_j, \tag{29}$$

respectively, where N is the number of QSS species and N_R the number of irreversible reactions. Note that unlike the previous reduction stages, this step requires all reactions to be irreversible. The reaction rate is calculated using

$$\Omega_j = k_j \prod_{k=1}^{N_S} x_k^{\nu'_{k,i}}, \tag{30}$$

where k_j is the Arrhenius rate coefficient, N_S the total number of species (both QSS and non-QSS), and x_k the molar concentration of the kth species. Equation (28) may be nonlinear due to the participation of multiple QSS species or a stoichiometric coefficient greater than one for a particular QSS species in a reaction. However, due to the typically low concentration of QSS species (after an initial transient), these nonlinear terms may not be important. This importance can be quantified by calculating the normalized contribution of the nonlinear terms to the production and consumption rates of the ith species, expressed as

$$\pi_i = \frac{\sum_{j=1}^{N_R} \nu''_{i,j} \Omega_j \delta_j}{\omega_{\mathrm{P},i}} \quad \text{and} \quad \kappa_i = \frac{\sum_{j=1}^{N_R} \nu'_{i,j} \Omega_j \delta_j}{\omega_{\mathrm{C},i}}, \tag{31}$$

respectively, where

$$\delta_j = \begin{cases} 1 & \text{if reaction } j \text{ involves} > 1 \text{ QSS reactant,} \\ 0 & \text{otherwise.} \end{cases} \tag{32}$$

These measures of importance are similar to those used in DRG/DRGEP as well as unimportant reaction elimination, and similarly if the values fall below a cutoff threshold the terms are considered unimportant. The nonlinear terms may be neglected if

$$\max_{k \in \{\mathscr{D}\}} \left(\max_{\text{all species } i,k} \pi_i \right) < \varepsilon_{\text{nonlin}} \quad \text{and} \quad \max_{k \in \{\mathscr{D}\}} \left(\max_{\text{all species } i,k} \kappa_i \right) < \varepsilon_{\text{nonlin}} \tag{33}$$

where k is a reaction state, $\{\mathscr{D}\}$ the set of all reaction states of interest, and $\varepsilon_{\text{nonlin}}$ a small user-defined threshold (e.g., 0.1–0.2). If Eq. (33) is satisfied, then the nonlinear contributions to QSS equations are deemed negligible and removed.

Once the nonlinear terms are eliminated, the QSS relations in Eq. (28) can be expressed using a system of linear equations, which Lu and Law [34] termed the linearized QSS approximation (LQSSA):

$$C_i x_i = \sum_{k \neq i} P_{ik} x_k + P_{i0} \quad i = 1, 2, \ldots, N \tag{34}$$

where

$$C_i = \frac{\omega_{\mathrm{C},i}}{x_i}, \tag{35}$$

$$P_{ik} = \frac{\sum_{j=1}^{N_R} \nu''_{i,j} \Omega_j \operatorname{sgn}\left(\nu'_{k,j}\right)}{x_k}, \tag{36}$$

$$P_{i0} = \sum_{j=1}^{N_R} \nu''_{i,j} \Omega_j \delta'_j, \tag{37}$$

$$\operatorname{sgn}\left(\nu'_{k,j}\right) = \begin{cases} 1 & \text{if } \nu'_{k,j} > 0, \\ 0 & \text{if } \nu'_{k,j} = 0, \end{cases} \quad \text{and} \tag{38}$$

$$\delta'_j = \begin{cases} 1 & \text{if reaction } j \text{ involves no QSS reactant,} \\ 0 & \text{otherwise.} \end{cases} \tag{39}$$

Note that the consumption and production coefficients C_i, P_{ik}, and P_{i0} are independent of QSS species concentrations, and either positive or zero. As with the initial nonlinear QSS relations, the system of equations given by Eq. (34) may be solved by iterative schemes, but could suffer the same computational difficulties. In addition, the system could be solved through the typical Gaussian elimination, but its algorithmic complexity is a cubic function of N. Instead, an analytic solution based on variable substitution and elimination offers an efficient approach for calculation the QSS species concentrations. Now, the challenge becomes finding the best order for elimination by substitution that minimizes the number of operations required. Lu and Law [34] proposed using graph theory to identify the interdependence of QSS species. We detail the construction of such a QSS graph (QSSG) in the following section.

The system of LQSSA equations, as given by Eq. (34), can be transformed to a form that offers a direct solution for each variable:

$$x_i = \sum_{k \neq i} A_{ik} x_k + A_{i0} \quad i = 1, 2, \ldots, N \tag{40}$$

where

$$A_{ik} = \frac{P_{ik}}{C_i} \quad \text{and} \quad A_{i0} = \frac{P_{i0}}{C_i} \tag{41}$$

In this formulation, the solution for the concentration x_i directly requires x_k if $A_{ik} > 0$. Similar to the concept used in DRG/DRGEP, the dependence of QSS species concentrations on one another can be mapped to a directed graph, where each QSS species is a graph node: the QSS graph (QSSG). Edges between nodes exist when there is a direct dependence between species: the edge $x_i \to x_k$ exists if and only if $A_{ik} > 0$. In some cases, Eq. (40) may be explicit for all QSS species—meaning there is no interdependence—and the equations can be solved in order without the need to substitute expressions and eliminate variables. In general, though, the QSSG will consist of strongly coupled groups of species that form cycles of dependence—these are known as the strongly connected components (SCCs) of the graph. Intergroup coupling, on the other hand, is acyclic, such that an explicit solution order of groups may be determined.

One important step is to prune the QSSG of unimportant edges, again in a similar manner to the elimination of unimportant species in the DRG and DRGEP methods. While less important when a small number of QSS species exist, trimming the edges in a large graph ensures that the matrix $\mathbf{A}$ formed by the A_{ik} coefficients is sparse, resulting in multiple groups—rather than one large cyclic group made up of all the QSS species. The importance of QSSG edges can be determined by calculating the normalized contribution of the kth QSS species to the production rate of the ith QSS species (not to be confused with the DRGEP direct interaction coefficient given by Eq. (1)):

$$r_{ik} = \max_{\{\mathscr{D}\}} \left(\frac{A_{ik} x_k}{\sum_{j \neq i} A_{ij} x_j + A_{i0}} \right) \tag{42}$$

where $\{\mathscr{D}\}$ indicates the maximum over all reaction states of interest. Unimportant QSSG edges are then identified and removed through comparison with a small cutoff threshold ε_{QSS}, such that the remaining edges satisfy

$$x_i \to x_k \iff r_{ik} \geq \varepsilon_{\text{QSS}}. \tag{43}$$

After pruning the graph edges, the next step is to identify the SCCs and perform a topological sort [28], which provides the order in which the SCCs are to be solved. This is performed using the

DIGRAPH_ADJ_COMPONENTS subroutine of Burkardt's GRAFPACK [35], with the algorithm originally taken from Thulasiraman and Swamy [36]. The adjacency matrix $\mathbf{E}$ of the QSSG, a necessary input, is formed by

$$E_{ik} = \begin{cases} 1, \text{if there is an edge } x_i \to x_k, \\ 0, \text{otherwise.} \end{cases} \tag{44}$$

With the SCCs identified and sorted, the only remaining task is to solve for the intra-SCC species concentrations through variable elimination by substitution. Lu and Law [34] proposed a method to identify a near-optimal sequence for variable elimination, by calculating the normalized expansion cost c_i of each variable x_i, defined as

$$\mathbf{c} = \mathbf{L}\mathbf{c} \tag{45}$$

where

$$\mathbf{c} = (c_1, c_2, \ldots, c_M)^{\mathrm{T}}, \quad \text{and} \tag{46}$$

$$L_{ik} = \frac{E_{ik}}{\sum_{j=1}^{M} E_{jk}}, \tag{47}$$

where M is the number of QSS species in the current SCC. Equation (45) is an eigenvalue problem, where the column vector $\mathbf{c}$ is the eigenvector of $\mathbf{L}$ associated with the principal eigenvalue. Practically, we solve this equation using the LAPACK subroutine DGEEV [32], and select the resulting eigenvector associated with the largest eigenvalue. The values of $\mathbf{c}$ represent the relative expansion cost of each QSS species in the SCC, such that species with lower c_i values should be eliminated from later expressions first. Therefore, species within the SCC are sorted in ascending order of c_i for elimination by substitution.

Finally, we note that in some cases, the LQSSA—and therefore the analytic QSS solution—may not be valid when the contributions from the nonlinear terms (π_i and κ_i) are not negligible. For example, Lu and Law [34] compared the terms' importance to detailed and skeletal mechanisms for ethylene, consisting of 70 and 33 species, respectively. They found that while the terms were in fact small (between 0.1–0.2) for the skeletal mechanism, the same was not true for the detailed mechanism, where the nonlinear contributions to the production rates (π_i) were nearly unity in some cases. It remains to be seen whether the LQQSA approximation is valid in the case of larger, more complex skeletal mechanisms resulting from even larger initial detailed mechanisms. When non-negligible nonlinear terms exist in the skeletal mechanism, two main options exist: (1) remove offending species from the QSS list, such that the nonlinear terms become negligible; and (2) develop a hybrid analytic-iterative solution scheme, where most of variables are calculated analytically and a small number of nonlinear terms are solved iteratively.

2.6 Reduction package

The various reduction stages described above are integrated into a new version of the Mechanism Automatic Reduction Software (MARS) package, first described by Niemeyer and Sung [16, 26]. This version uses VODE_F90 [37], a Fortran 90 version of the well-known VODE solver, in conjunction with CHEMKIN-III [38] to generate numerical solutions of constant volume autoignition

using the detailed reaction mechanism over the range of initial conditions for the desired coverage of the skeletal mechanism. Chemical kinetics data used in the reduction procedure are sampled densely around the ignition evolution. In addition, the ignition delay results from the detailed mechanism are used to measure the error of skeletal mechanisms.

MARS first employs the DRGEPSA with a user-defined error limit and the iterative threshold technique described previously automatically generate a skeletal mechanism with a minimal number of species. Next, the unimportant reaction elimination stage is performed to further reduce complexity of the skeletal mechanism by removing reactions in addition to those eliminated with unimportant species. This skeletal mechanism is converted to a version with only irreversible reactions using the freely-available tool irrev_mech [39]. Then, using the resulting skeletal mechanism, a CSP-based time scale analysis algorithm identifies global QSS species. Finally, MARS generates analytical solutions for the concentrations of these QSS species. The final reduced mechanism consists of a CHEMKIN-format mechanism file containing the non-QSS species, and a Fortran 90 source file containing a replacement for the CHEMKIN subroutine CKWYP, which calculates the molar production rates of the species.

The MARS code is parallelized using OpenMP [40], such that multiple autoignition simulations may be performed simultaneously. This greatly reduces the run time of the original sampling of the detailed mechanism, in addition to the sensitivity analysis portion of the DRGEPSA stage.

3 Results and Discussion

We generated skeletal and reduced mechanisms at various levels of detail from a detailed mechanism for gasoline surrogates of Mehl et al. [3], which consists of 1389 species and 5936 reversible reactions. Thermochemical data were sampled from constant volume autoignition simulations performed over the range of conditions listed in Table 1, using the surrogate formulation of Mehl et al. [3]: 48.8% *iso*-octane, 15.3% *n*-heptane, 30.6% toluene, and 5.3% 2-pentene (by molar percentage). This range of conditions was chosen to sample over a wide range of temperatures, pressures, and species compositions relevant to HCCI engine conditions, while limiting the computational cost of the reduction procedure. We selected error limits of 10% and 30% to produce two pairs of skeletal and reduced mechanisms at different levels of detail, and chose *iso*-octane, *n*-heptane, toluene, 2-pentene, oxygen, and nitrogen (to prevent removal) as the DRGEP target species.

Table 2 shows the results for the various stages of the reduction procedure, for both error limits. Both the final skeletal (following the reaction elimination stage) and reduced mechanisms represent significant reduction from the initial detailed mechanism. The iterative threshold algorithm of the DRGEP algorithm selected cutoff thresholds ($\varepsilon_{\mathrm{EP}}$) of 0.007 and 0.019 for the 10% and 30% error limits, respectively. The separation values ε^* used in the sensitivity analysis were 0.01 and 0.11. For the reaction elimination stage, the $\varepsilon_{\mathrm{reac}}$ threshold values 0.007 and 0.01 were selected.

Next, in the CSP analysis, safety factors (α_{CSP}) of 100 and CSP threshold $\varepsilon_{\mathrm{CSP}}$ values of 0.0001 were used for both cases. For both, the maximum contributions of the nonlinear terms were quite small: $\pi_{\mathrm{max}} = 6.8\times10^{-16}$ and $\kappa_{\mathrm{max}} = 4.2\times10^{-6}$ for the 10%, and $\pi_{\mathrm{max}} = 2.6\times10^{-18}$ and $\kappa_{\mathrm{max}} = 8.7\times10^{-4}$ for the 30% skeletal mechanisms. Interestingly, the skeletal mechanism generated using the tighter error control (10%) is over 150% larger than the slightly less accurate version (30%); a similar relationship is exhibited between the number of QSS species.

Equivalence Ratio	Initial Temperature (K)	Initial Pressure (atm)
1.0	800	10
1.0	750	60
0.6	1200	60
0.6	1100	10
0.6	1000	60
0.6	800	10
0.6	750	10
0.6	750	60
0.2	800	60
0.2	700	20
0.2	800	20

Table 1: Set of initial conditions used to generate skeletal mechanisms for gasoline surrogates. Adopted from that used by Mehl et al. [4].

Error limit	Stage	# Species	# Reactions
10%	DRGEP	471	2434
	SA	423	2131
	Reac. elim	423	1747
	Reduced	245 (178 QSS)	3448
30%	DRGEP	341	1727
	SA	270	1237
	Reac. elim	270	1001
	Reduced	178 (92 QSS)	1965

Table 2: Skeletal and reduced mechanisms sizes for gasoline surrogates. The reduced mechanisms consist of more reactions since all reversible reactions were converted into two irreversible reactions.

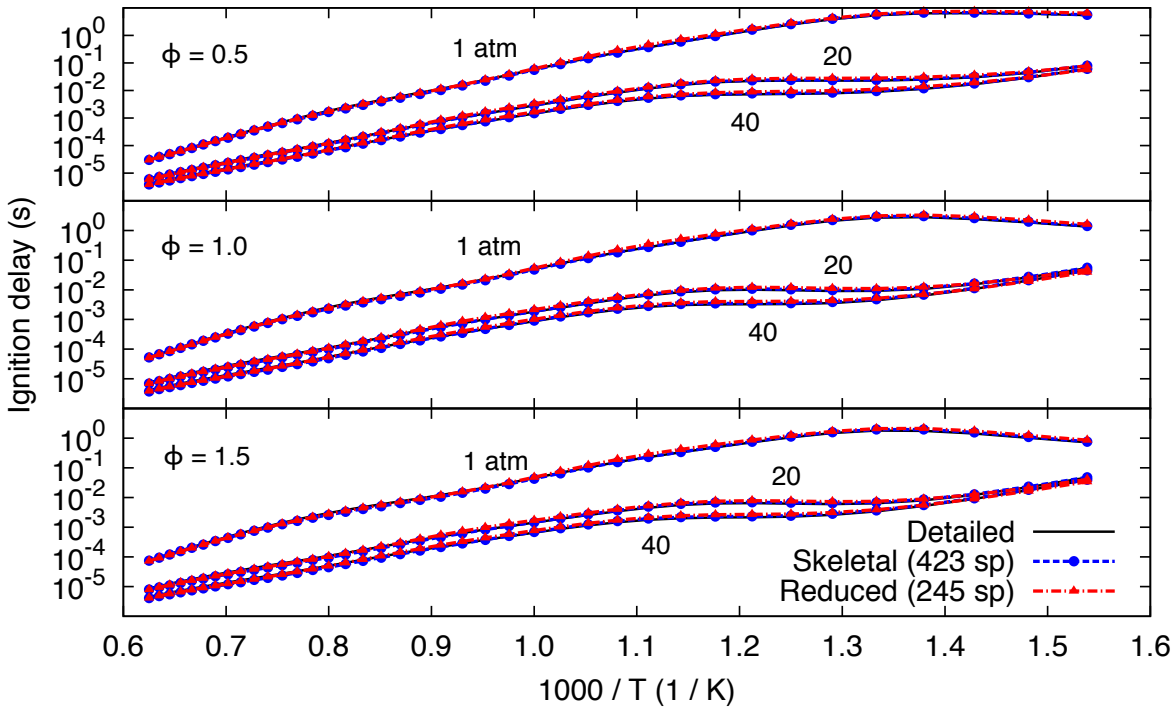

Figure 1: Autoignition validation of the skeletal and reduced mechanisms for gasoline, corresponding to a 10% error limit, over a range of initial temperatures and pressures, and at varying equivalence ratios.

Validation of the skeletal and reduced mechanisms was performed with constant volume autoignition simulations over a range of initial conditions for temperature, pressure, and equivalence ratios. The results for the mechanisms generated with the 10% and 30% error limits are presented in Figs. 1 and 2, respectively. Both the skeletal and reduced mechanisms generated using the tighter error control predicted the ignition delay of the detailed mechanism extremely well, with little discernible discrepancies. The mechanisms associated with the 30% error limit performed nearly as well, with some error in the negative temperature coefficient region.

We note that the QSS reduction parameters (α_{CSP} and ε_{CSP}) were chosen based on trial and error. Lu and Law [13, 31] used "jumps" in the numbers of QSS species as a function of ε_{CSP} to select the best values for methane and *n*-heptane reduced mechanisms (0.1 in both cases). Figure 3 shows this relationship for the current situation, for the skeletal mechanism with 270 species (30% error). While similar jumps in number are observed, we found that more care must be taken in selecting ε_{CSP}. For example, using a value of 0.001 results in a reduced mechanism with 138 non-QSS and 132 QSS species. Even though this value represents a point in Fig. 3 prior to a jump, the resulting reduced mechanism does not perform well, as demonstrated in Fig. 4. A more systematic approach to determining the optimal ε_{CSP} values is warranted, which will be pursued in future work.

4 Conclusions

Skeletal and reduced mechanisms for gasoline surrogates were generated using a combined strategy of skeletal reduction via the DRGEPSA method, followed by further unimportant reaction

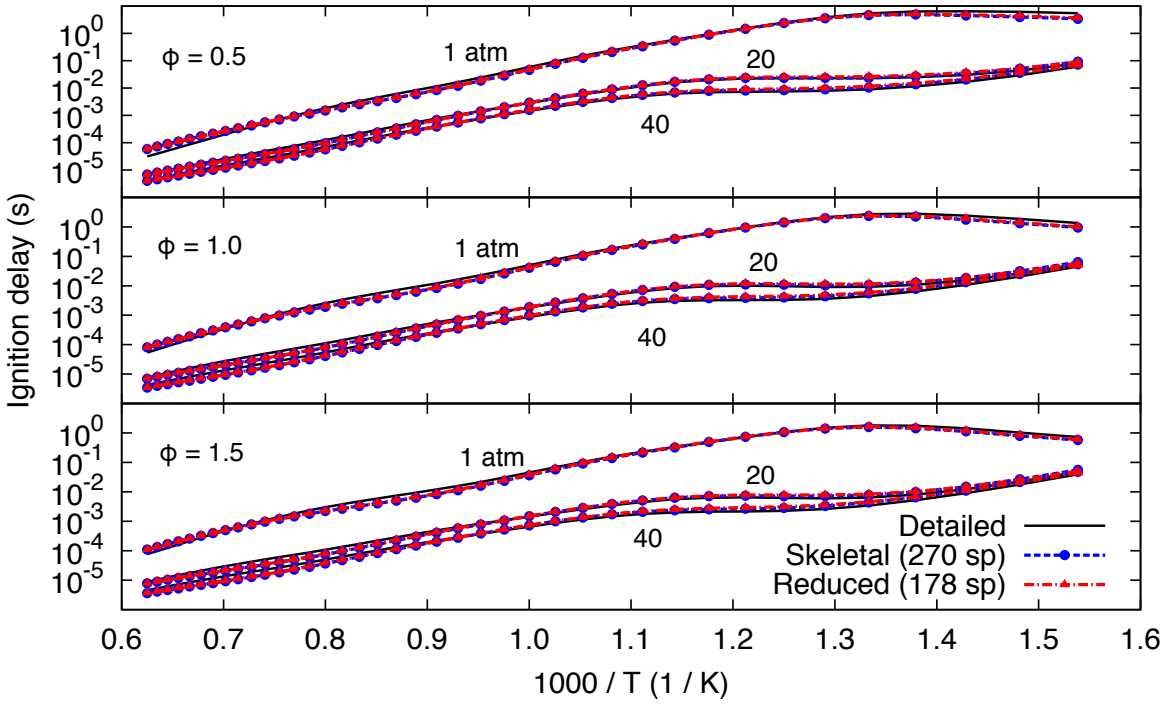

Figure 2: Autoignition validation of the skeletal and reduced mechanisms for gasoline, corresponding to a 30% error limit, over a range of initial temperatures and pressures, and at varying equivalence ratios.

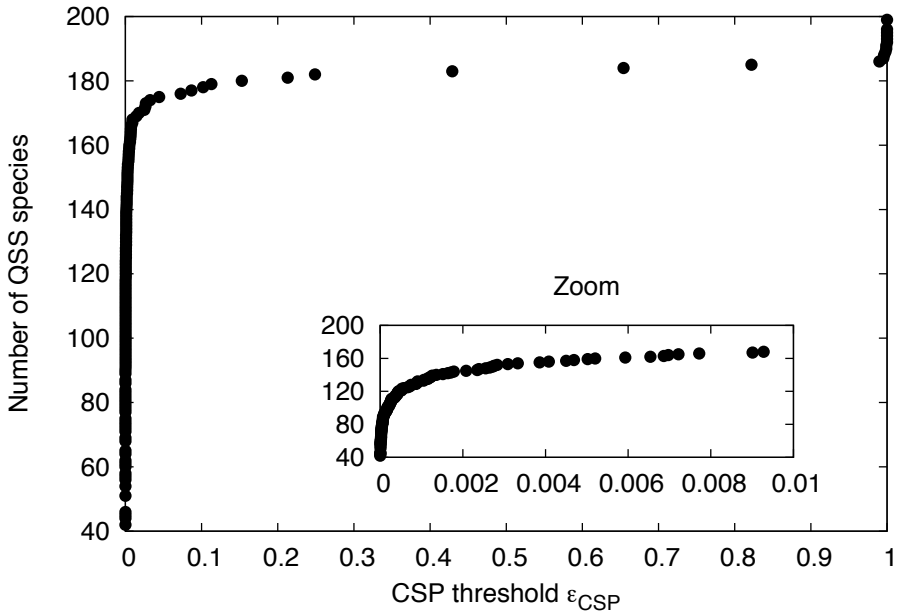

Figure 3: Number of QSS species as a function of CSP threshold, for the skeletal mechanism with 270 species generated using a 30% error limit.

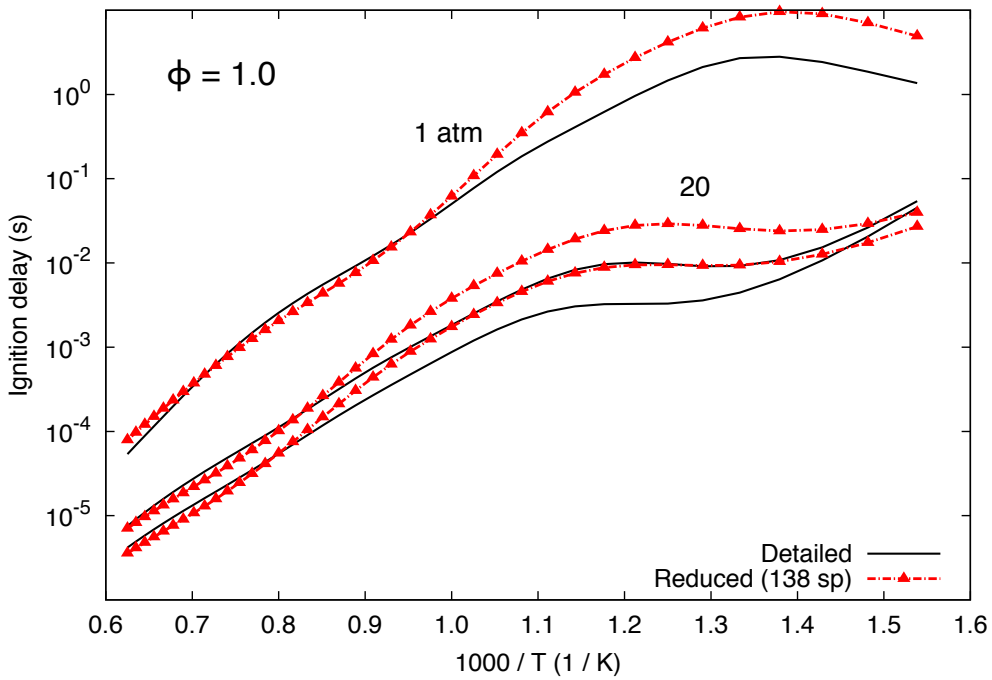

Figure 4: Comparison of autoignition delays between the detailed mechanism and a reduced mechanism with 138 non-QSS species (generated from the 30% error skeletal mechanism) for gasoline, over a range of initial temperatures and pressures, and at stoichiometric conditions.

elimination, then time-scale reduction based on the QSS assumption using CSP analysis. Using error limits of 10% and 30%, reduced mechanisms with 245 and 178 species, respectively, were generated from the original detailed mechanism with 1389 species. Validation of both reduced mechanisms showed good performance in predicting homogenous autoignition delay over a wide range of conditions. However, further validation is warranted, comparing the prediction of extinction limits and laminar flame speeds. In addition, detailed validation using HCCI engine simulations will be performed, determining the performance in predicting species profiles and heat release. Finally, additional investigation is needed in selecting the optimal cutoff threshold for CSP analysis, as methods used previously may result in a poorly performing reduced mechanism.

Acknowledgments

This work was supported by the National Science Foundation under Grant No. 0932559 and the National Science Foundation Graduate Research Fellowship under Grant No. DGE-0951783.

References

[1] M. Chaos, Z. Zhao, A. Kazakov, P. Gokulakrishnan, M. Angioletti, and F.L. Dryer. A PRF+toluene surrogate fuel model for simulating gasoline kinetics. In *5th US Combustion Meeting*, number E-62, March 2007.

[2] B M Gauthier, D F Davidson, and R K Hanson. *Combust. Flame*, 139 (2004) 300–311.

[3] Marco Mehl, William J Pitz, Charles K Westbrook, and Henry J Curran. *Proc. Combust. Inst.*, 33 (2011) 193–200.

[4] Marco Mehl, Jyh-Yuan Chen, William J Pitz, S M Sarathy, and Charles K Westbrook. *Energy Fuels*, 25 (2011) 5215–5223.

[5] G Kukkadapu, Kamal Kumar, Chih Jen Sung, Marco Mehl, and William J Pitz. *Proc. Combust. Inst.*, 34 (2013) 345–352.

[6] Tianfeng Lu and Chung K Law. *Prog. Energy Comb. Sci.*, 35 (2009) 192–215.

[7] Tianfeng Lu and Chung K Law. *Proc. Combust. Inst.*, 30 (2005) 1333–1341.

[8] Tianfeng Lu and Chung K Law. *Combust. Flame*, 144 (2006) 24–36.

[9] Tianfeng Lu and Chung K Law. *Combust. Flame*, 146 (2006) 472–483.

[10] AB Bendtsen, Peter Glarborg, and K Dam-Johansen. *Comput. Chem.*, 25 (2001) 161–170.

[11] Ramanan Sankaran, Evatt R Hawkes, Jacqueline H Chen, Tianfeng Lu, and Chung K Law. *Proc. Combust. Inst.*, 31 (2007) 1291–1298.

[12] X L Zheng, Tianfeng Lu, and Chung K Law. *Proc. Combust. Inst.*, 31 (2007) 367–375.

[13] Tianfeng Lu and Chung K Law. *Combust. Flame*, 154 (2008) 153–163.

[14] Perrine Pepiot-Desjardins and Heinz Pitsch. *Combust. Flame*, 154 (2008) 67–81.

[15] Kyle E Niemeyer and Chih-Jen Sung. *Combust. Flame*, 158 (2011) 1439–1443.

[16] Kyle E Niemeyer, Chih-Jen Sung, and Mandhapati P Raju. *Combust. Flame*, 157 (2010) 1760–1770.

[17] Wenting Sun, Zheng Chen, Xiaolong Gou, and Yiguang Ju. *Combust. Flame*, 157 (2010) 1298–1307.

[18] Max Bodenstein. *Z. Phys. Chem.*, 85 (1913) 329–397.

[19] DL Chapman and LK Underhill. *J. Chem. Soc., Trans.*, 103 (1913) 496–508.

[20] Sidney W Benson. *J. Chem. Phys.*, 20 (1952) 1605–1612.

[21] John D Ramshaw. *Phys. Fluids*, 23 (1980) 675–680.

[22] S H Lam and D A Goussis. *Proc. Combust. Inst.*, 22 (1988) 931–941.

[23] S H Lam. *Combust. Sci. Technol.*, 89 (1993) 375–404.

[24] S H Lam and D A Goussis. *Int. J. Chem. Kinet.*, 26 (1994) 461–486.

[25] Ulrich Maas and Stephen B Pope. *Combust. Flame*, 88 (1992) 239–264.

[26] Kyle E Niemeyer. Skeletal mechanism generation for surrogate fuels. MS thesis, Case Western Reserve University, 2010.

[27] Kyle E Niemeyer and Chih-Jen Sung. Mechanism reduction strategies for multicomponent gasoline surrogate fuels. In *7th NCM*, March 2011.

[28] Thomas H Cormen, Charles E Leiserson, Ronald L Rivest, and Clifford Stein. *Introduction to Algorithms*. The MIT Press, Cambridge, Massachusetts, 3rd edition, 2009.

[29] Tianfeng Lu, Yiguang Ju, and Chung K Law. *Combust. Flame*, 126 (2001) 1445–1455.

[30] D A Goussis and S H Lam. *Proc. Combust. Inst.*, 24 (1992) 113–120.

[31] Tianfeng Lu and Chung K Law. *Combust. Flame*, 154 (2008) 761–774.

[32] E. Anderson, Z. Bai, C. Bischof, S. Blackford, J. Demmel, J. Dongarra, J. Du Croz, A. Greenbaum, S. Hammarling, A. McKenney, and D. Sorensen. *LAPACK Users' Guide*. Society for Industrial and Applied Mathematics, Philadelphia, PA, 3rd edition, 1999.

[33] Chung K Law, Chih Jen Sung, Hai Wang, and Tianfeng Lu. *AIAA J.*, 41 (2003) 1629–1646.

[34] Tianfeng Lu and Chung K Law. *J. Phys. Chem. A*, 110 (2006) 13202–13208.

[35] John Burkardt. GRAFPACK. http://people.sc.fsu.edu/~jburkardt/f_src/grafpack/grafpack.html, September 2006.

[36] K Thulasiraman and M N S Swamy. *Graphs: Theory and Algorithms*. John Wiley & Sons, Inc., New York, 1992.

[37] George D Byrne and Skip Thompson. VODE_F90. www.radford.edu/~thompson/vodef90web, March 2006.

[38] Robert J Kee, Fran M Rupley, Ellen Meeks, and James A Miller. CHEMKIN-III: A FORTRAN chemical kinetics package for the analysis of gas-phase chemical and plasma kinetics. Technical Report SAND96-8216, Sandia National Laboratories, May 1996.

[39] Kyle E Niemeyer. irrev_mech. https://github.com/kyleniemeyer/irrev_mech, March 2013.

[40] OpenMP Architecture Review Board. OpenMP application program interface version 3.0. http://www.openmp.org/mp-documents/spec30.pdf, May 2008.